Materials Research. 2017; 20(1): 264-270
DOI: http://dx.doi.org/10.1590/1980-5373-MR-2015-0694

Green Synthesis of Gold Nanoparticles Using *Sumac* Aqueous Extract and Their Antioxidant Activity

Hoda Shabestarian[a], Masoud Homayouni-Tabrizi[b], Mozhgan Soltani[c], Farideh Namvar[d,e], Susan Azizi[f]*, Rosfarizan Mohamad[d,f], Hanieh Shabestarian[b]

[a] *Department of Basic Sciences, Faculty of Veterinary Medicine, Ferdowsi University of Mashhad, Mashhad, Iran*
[b] *Department of Biochemistry and Biophysics, Mashhad Branch, Islamic Azad University, Mashhad, Iran*
[c] *Department of Biology, Mashhad Branch, Islamic Azad University, Mashhad, Iran*
[d] *Institute of Tropical Forestry and Forest Products – INTROP, Universiti Putra Malaysia, Serdang, Selangor, Malaysia*
[e] *Research Center for Animal Development Applied Biology, Mashhad Branch, Islamic Azad University, Mashhad, Iran*
[f] *Department of Bioprocess Technology, Faculty of Biotechnology and Biomolecular Sciences, Universiti Putra Malaysia, Serdang, Selangor, Malaysia*

Received: November 17, 2015; Revised: November 8, 2016; Accepted: November 21, 2016

Green synthesis of nanoparticles which have eco-friendly favourable solvent systems and environmentally reducing agents is of excessive importance. In this paper, we aimed to develop environmentally friendly, rapid and simple producer for the synthesis gold nanoparticles (Au-NPs) using aqueous extract of *sumac* as reducing agents for gold ions as well capping agent for the bio-formed Au-NPs. The bio-synthesized Au-NPs were characterized by the UV-visible spectroscopy, FTIR, TEM, and zeta-potential measurements. The surface plasmon resonance band centred at 520 nm for Au-NPs was characterized by UV-visible spectrophotometer. The probable bio-molecules are polyphenols may responsible for reduction of gold ions were recognized through FT-IR. The TEM result shows the bioformed Au-NPs are spherical in shapes with the mean size of 20.83 ±4.4 nm. The capping of anionic bio-molecules on the surface of Au-NPs was confirmed by zeta potential assessment (-25.3 mV) and is responsible for the electrostatic stability. In vitro antioxidant activity studies showed that DPPH (2,2-diphenyl-1-picrylhydrazyl) and ABTS (2, 2'-azino-bis 3-ethylbenzthiazoline-6-sulfonic acid) activities increased in a dose dependent manner. The bio-synthesized nanoparticles can potentially useful in pharmaceutical and biomedical applications.

Keywords: *Green synthesis, plant extract, Sumac, gold nanoparticles*

1. Introduction

Nanotechnology has underpinned new scientific growths with novel materials which display new properties quite different from their bulk counterparts. Nanotechnology is a multi-disciplinary field, which covers a vast and diverse array of devices derived from engineering, biology, physics and chemistry[1]. Recently, there is a rising interest to develop eco-friendly gentle nanoparticle synthesis procedure which does not utilize any toxic materials in the production. Nanoparticles are solid structures with a size less than100 nm and have found their applications in optoelectronics, catalysis, imaging, sensing, and in drug and gene delivery[2]. Between the nano-sized particles, Au-NPs have merited main attention owing to their exclusive and tunable Surface Plasmon Resonance (SPR) [3]. It has many efficient biomedical applications including drug delivery, tissue/tumor imaging, photothermal therapy, and immunochromatographic identification of pathogens in medical samples[4]. It has as well as other uses such as colorimetric procedures and for the determination of heavy metallic ions in aqueous solution[5]. The advantages of gold nanoparticles originate from their safety, biocompatibility and capability to target delivery of therapeutic agents[6]. The synthesis of Au-NPs is a growing research area owing to the potential uses for the growth of new technologies.

Several physical and chemical approaches have been used for the conventional Au-NPs synthesis, such as pyrolysis, chemical reduction, laser ablation, sol gel, chemical or physical lithography electro-deposition, vapor deposition, most of these methods being costly, and/or wanting the use of toxic solvents[7-9]. Though, these approaches not only use costly and hazardous chemicals reagents as reducing and capping agents, but it is very probable which residual unreacted harsh reagents and by-products make Au-NPs so

* e-mail: azisusan@gmail.com

formed inappropriate for use in biomedical applications. To overcome these methods and use of toxic reducing agents, the attention in this area has moved towards 'green' chemistry for preparation of nanoparticles. Among green methods are those concerned with plant[10,11], bacteria[12], fungi[13], enzymes[14] and algae[15]. These biosynthesis methods are currently under extensive exploration. Because of their amenability to biological functionalization, the bio-synthesized nanoparticles offer many benefits of eco-friendliness and compatibility for biomedical and pharmaceutical applications[16].

Sumac, (Rhuscoriaria L., family Anacardiaceae) which grows wild in the district spreading from the Canary Islands over the Mediterranean coastline to Iran and Afghanistan, is endemic to the Mediterranean and Southeastern Anatolian areas of Turkey[17]. The fruit extracts of *sumac* have been reported to contain flavonols, phenolic acids, hydrolysable tannins, anthocyannins and organic acids for example malic, citric and tartaric acids[18-20]. In addition, *sumac* has a high level of antioxidants such as tannins and phenolic compounds.[18,21]. These antioxidants compounds can be introduced on the surface of nanoparticles throughout the nanoparticles fabrication process which finally leads to arising consequent surface effects during their application Therefore, stable metallic nanoparticles synthesized with *sumac* could be highly useful for cancer therapy.

In this paper, we present a rapid, simple method of Au-NPs synthesis by reducing aqueous salt solutions of gold using *Sumac* extract, without any extra additive protecting nanoparticles from aggregating. The present synthetic green process provides nanosized particles with narrow size distribution. Study of antioxidant efficiency of this green nanoparticles using ABTS and DPPH radical scavenging assay is an important in-vitro analysis which in both methods decolorization assays apply to identify the existence of antioxidant. In most of the assays to determine the antioxidant properties, the ABTS activity was strongly correlated with DPPH because both methods are responsible for the same chemical property of H^- or electron-donation to the antioxidant. The green nanoparticles showed good antioxidant activity in radical scavenging ABTS and DPPH analysis. The process can be also applied for production of other metallic nanocrystalline with biomedical properties.

2. Materials and Methods

2.1. Materials

Red *Sumac* powder was bought in bulk from local market in Iran.

Hydrogen tetrachloroaurate (III) ($HAuCl_4\,3H_2O$, 99.98 %), which was used as a gold precursor, was supplied by Sigma-Aldrich (St. Louis, MO, USA). All the solutions were prepared with deionized water.

2.2. Preparation of Sumac Extracts

1 g of *Sumac* was dispersed in 100 mL distilled water under gentle stirring and heated at 100 °C about 30 min. Then extract was filtered through mesh, followed by Millipore filter (0.2 μm), and kept at −20 °C before apply.

2.3. Biosynthesis of Au-NPs

A volume of 50 mL of 0.1 mM $HAuCl_4\,3H_2O$ solution was reacted with 50 mL of the aqueous extract of *sumac* for 40 min under continuous stirring at 40 °C and then permitted to stand at ambient temperature for another 1 h. The purple solid product was separated from solution through centrifugation at 8000 rpm for 15 min and washed carefully with distilled water. The final sample was achieved by drying at 45˚C.

2.4. Characterization of Au-NPs

Phase purity were determined by X-ray diffraction (XRD) analysis recorded by diffractometer (XPERT-PRO) with nickel-filtered Cu (λ = 1.542 Å) at 40 kv and 30 mA. The mean particle size of nanoparticles was determined based on the XRD pattern according to the line width of the (1 1 1) peak through the Debye–Scherrer method. The chemical structure of the dried samples were examined at wavenumber range from 400 to 4000 cm^{-1} by using FTIR spectrometer (Perkin-Elmer 1725X, Waltham, MA, USA), The morphology and size of the sample was observed using a Hitachi (Tokyo, Japan) H-7100 electron microscope at120 kV. The mean size and particle size distribution of 70 nanoparticles were evaluated on the basis of three TEM images with the assistance of Sigma-Scan Pro software (SPSS IBM, Statistics 20, IBM Corporation, Endicott, NY, USA). The UV–Visible absorption of samples was observed using UV–Vis spectrophotometer (a Lambda 25-Perkin Elmer, Waltham, MA, USA) in the range of 200–800 nm. The laser Doppler electrophoresis method was applied to analyse the particle electrostatic charge, in which 100 μl of the solution was diluted with 1.5 ml of distilled water and located into a cuvette of the Zeta sizer-nano instrument (Malvern, UK); the results are expressed as zeta potential (ZP). The assessments were carried out at a pH of 7.26 ± 0.13 to mimic physiological pH.

2.4.1. DPPH Radical Scavenging Assay

Free radical scavenging activity of nanoparticle was evaluated by using its ability to trap the 2,2-diphenyl-1-picrylhydrazyl (DPPH) free radicals. Different concentrations (25-800 μM) of biosynthesized Au-NPs (Au-NPS/*sumac*) were added, in equal volume, to 0.1 mM methanolic DPPH solution. After 30 min incubation at room temperature

absorbance of sample was read at 517 nm. Glutation (GSH) was used as a standard compound [22].

2.4.2. ABTS Radical Scavenging Assay

ABTS (2, 2'-azino-bis 3-ethylbenzthiazoline-6-sulfonic acid) free radical scavenging activity was analysed according to the method described by Li, et al 2011 [23] with moderate modifications. Briefly, ABTS•+ stock solution was prepared by mixing 7 mM of ABTS and 2.45 mM of potassium persulfate and incubation at room temperature for 12-16 h. The ABTS·+ working solution was prepared by dilution of the ABTS•+ stock solution and distilled water to gain a 0.70±0.02 absorbance at 734 nm. The reaction mixture was prepared by mixing 1 mL of the working solution in 1mL of various concentrations of nanoparticle. After incubation for 1 h at room temperature in dark, absorbance was taken at 734 nm.

The experiments were done in triplicate and results were expressed as mean ± SD. Statistical analyses were done using SPSS version 20.0 (SPSS Inc., Chicago, USA). Data were initially evaluated for homogeneity of variance and normality. Probability values of less than alpha ($P \leq 0.05$) were considered statistically significant.

3. Results and Discussion

3.1. UV analysis

The detailed analysis on the *sumac* bioformed of Au-NPs was carried out in this study. Figure 1 shows the change in colour of reaction mixture at beginning, mid and end point of time of the reaction. The colour of medium was altered from agate red to light ruby red after 30 min and then to dark purple after 1 h of incubation signified the completed formation of Au-NPs. The change in colour of the medium was considered by visual inspection.

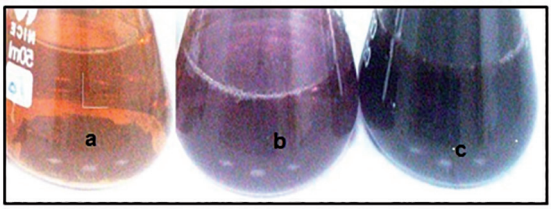

Figure 1: Synthesis of Au-NPs using aqueous extract of *sumac* at A) initial, B) 30 min and C) 1 hour of the reaction time

It was noticed that the reduction of the $AuCl_4^-$ ions during exposure to *sumac* solution and formation of gold nanoparticles can be easily followed by UV–vis spectroscopy. It has been established that the appearance of light ruby colour was owing to excitation of Surface Plasmon Resonances (SPR), characteristic of gold nanoparticles and gives rise to an absorption band at 510–540 nm [24]. The UV–vis spectra of reaction mixture obtained after 30 min of reaction was presented in Figure 2. Absorption spectra of Au-NPs exhibited a well-defined SPR's band centred at around 530 nm. The increase in intensity of absorption was owing to increasing number of nanoparticles formed because of reduction of gold ions existing in the aqueous solution. It is observed that Au-NPs band remained near to 530 nm even after 24 h of incubation suggests that the particles were well dispersed in the solution and there was not much aggregation [25].

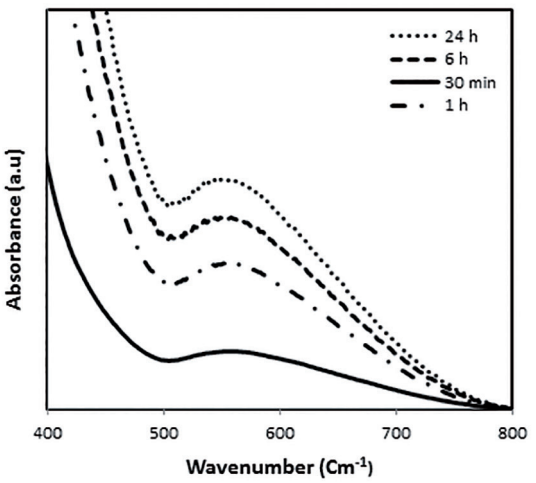

Figure 2: UV-visible spectra of bio-synthesized Au-NPs.

3.2. XRD analysis

The XRD pattern Au-NPs is shown in Figure 3 biosynthesized using *sumac* aqueous solution. A number of Bragg reflections with 2θ values of 38.12˚, 44.34˚, 64.28˚, and 77.63˚ which correspond to the (111), (200), (220), and (311) sets of lattice planes are detected which can be indexed to the face-centred cubic structures for gold. The data achieved matched with the database of the Joint Committee on Powder Diffraction Standards (JCPDS) file No. 04-0783. The widening of Bragg's peaks signifies the formation of nanoparticles. The sharp peaks signify some bio-organic compounds present in the nanoparticle during the synthesis [26].

Mean crystallite diameter of Au-NPs was calculated from the XRD pattern according to the line width of the (1 1 1) peak through the Debye–Scherrer equation.

$$L = \frac{k\lambda}{\beta \cos\theta}$$

where L is the particle size (nm), k is the Scherrer constant, β is the full width half maximum, θ is half of Bragg angle and λ is the wavelength of X-ray . The particle size of the Au- NPs was around 16 nm.

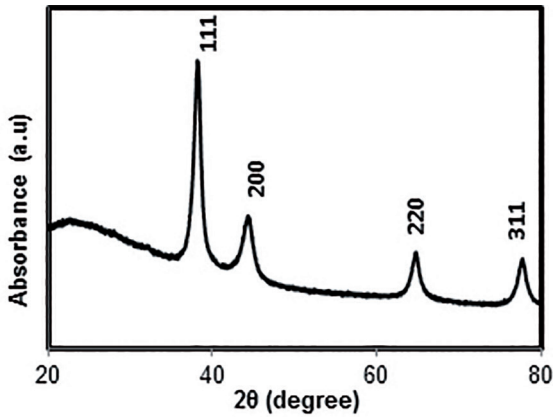

Figure 3: XRD pattern of bioformed Au-NPs

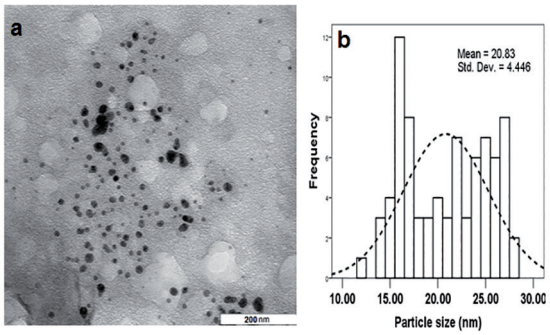

Figure 4: TEM image (a) and particle size distributions (b) of biosynthesized nanoparticles

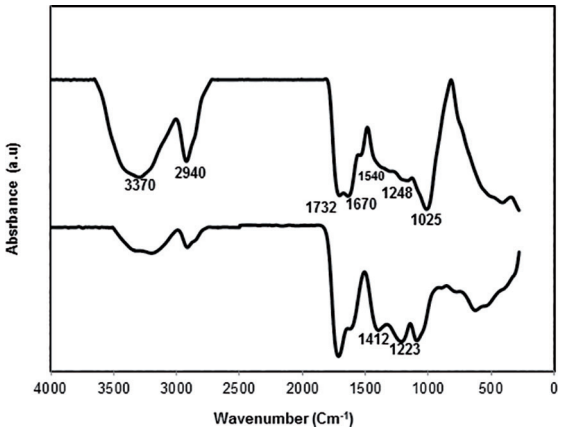

Figure 5: FTIR spectroscopic analysis of *sumac* extract (a) and bioformed Au nanoparticles (b)

3.3. TEM observations

The TEM image Figure 4a and particle size distribution diagram Figure 4b display the Au-NPs formed were well dispersed with spherical structures and a bi-medial distribution between two main populations of nanoparticles near 15 and 25 nm. The mean particle size of obtained nanoparticles was 20.83 with some deviations. The difference in the obtained values of the particle size of the Au- NPs is due to the fact that TEM measurements are based on the difference between the observable particle edges, while XRD calculations measure the extended crystalline region that diffracts X-rays coherently. Therefore, the XRD technique has a further accurate measure and leads to smaller sizes[27]. The particles are extremely mono-disperse this could be owing to the fact that the existence of some significant bio-organic molecules in the plant extract seems to act as a ligand which efficiently stabilizes the formed gold nanoparticles and thus controlling nanoparticle growth and clustering. Alternatively, it is possible that the biomolecules present in the *sumac* extract were believed to be the agents responsible for reducing the Au^{+} to Au°.

3.4. FTIR analysis

The FTIR spectra of untreated and treated *sumac* extract sample containing Au-NPs are illustrated in Figure 5. The untreated *sumac* sample shows absorption bands at 3370, 2940, 1723, 1670 and 1540, 1248, and 1025 cm^{-1} which assigned to –OH stretching vibration, –CH and $–CH_2$ vibration of aliphatic hydrocarbon, carbonyl group (C=O), aromatic ring stretching vibration and ethereal C-O asymmetric stretching vibration arising from the pyran-derived ring structure of condensed tannins, respectively [28]. The observed signals were more specific of flavonoids and tannins which are very plentiful in *sumac* extract. For untreated sample the strongest absorption band can be assigned to hydroxyl peak (O-H stretching) at 3370 cm^{-1}, which may be responsible for the reduction of metal ion to metal nanoparticles. The reduction of typical corresponding peak of hydroxyl groups and appearance of strong carbonyl peak suggest the oxidation process of fruit metabolites [29,30]. This band more occur in tannins and other phenolic compounds indicating the participation of these biomolecules in the synthesis of Au-NPs. Gold exists as $AuCl_4^-$ in solution which is a very strong oxidizing agent and could thus help in reduction of Au(III) to Au(0) [31]. Tannins and other phenolic compounds were oxidized in the presence of $AuCl_4^-$ and thus hydroxyl groups converted to carbonyl groups. The π electrons of carbonyl groups (C=O) from these biomolecules in a Red/Ox system can transfer to the free orbital of metal ions and convert that to the metallic particles (Figure 6). The bonds between carbonyl groups and metal ion give a well-known signature in the FT-IR spectrum. After formation of gold nanoparticles the shift in the peak at 1723 is attributed to the binding of carbonyl group with nanoparticles. Moreover, the FT-IR of extract after formation of Au-NPs shows additional signals at 1412 and 1223 cm^{-1} signifying the formation of new bonds between metallic nanoparticles and functional groups of biomolecules present in *sumac* extract. Therefore it can be supposed that these compounds like flavonoid, tannins and other phenolic compounds acts as the capping agent in the formation of gold nanoparticles which similarly help in the

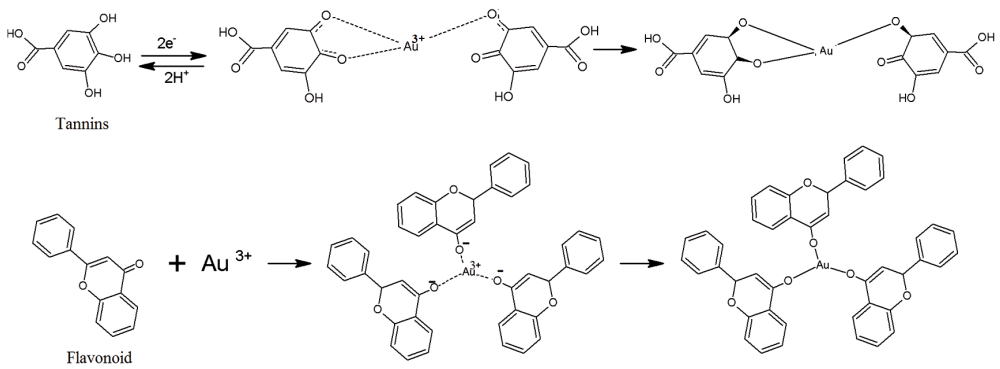

Figure 6: Reducing capability tannins and of flavonoid to produce Au-NPs

stabilization of nanoparticles at physiological condition[32]. Similar result was also reported in our pervious study for synthesizing of silver nanoparticles[33].

3.5. Zeta potential analysis

A High absolute zeta potential value indicates a high electric charge on the surface of the NPs. It describes strong repellent forces among the particles, preventing aggregation and stabilizing NPs in the buffer solution. In natural conditions (pH close to 7.2), the values of zeta potential of Au-NPs were equal to -25.3 mV (Figure 7). It could be concluded that gold nanoparticles had warped with anionic compounds and that the particles were fairly stable due to the electrostatic repulsion [34].

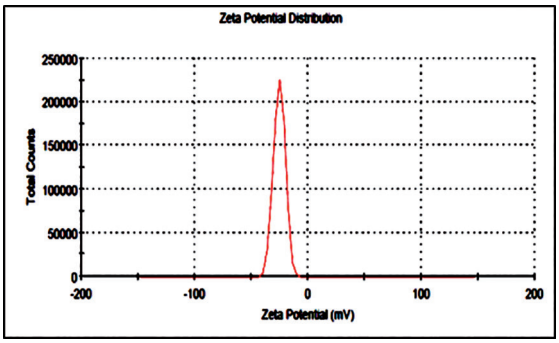

Figure 7: Zeta potential of biosynthesized Au-NPs

3.6. DPPH Radical Scavenging Activity

The 2,2-diphenylpicrylhydrazyl (DPPH) assay is widely used in antioxidants to evaluate the properties of compounds for scavenging free radicals. The method is based on the spectrophotometric measurement of the DPPH concentration change resulting from the reaction with an antioxidant. ABTS assay is based on inhibition of the production of the ABTS radical cation did not involve a substrate. ABTS with an absorption maximum at 342 nm has high water solubility and chemical stability. It is a peroxidase substrate which, when oxidized in the presence of H_2O_2 generates a metastable radical cation with a characteristic absorption spectrum and high molar absorptivity at 414 nm. DPPH is pure radical scavenging whereas ABTS measures both HAT (Hydrogen atom transfer) and SET (Single electron transfer). In this study we used both methods.

The free radical scavenging activity of biosynthesized Au-NPs was examined by DPPH scavenging. The NPs showed a dose dependent activity and the DPPH scavenging effect was 13.43% at a concentration of 25µM and then reached to the 85.73% at 800 µM of Au-NPs (Figure 8). Nanoparticle displayed good inhibitory effect on DPPH free radical. Many kinds of antioxidants of the extract could perform synergistically. During the synthesis of the Au-NPs, these bio- compounds are adsorbed onto the surface of the Au-NPs. Considering the high surface area to volume ratio, it appears that these Au-NPs, show a high tendency to interact with and reduce DPPH.

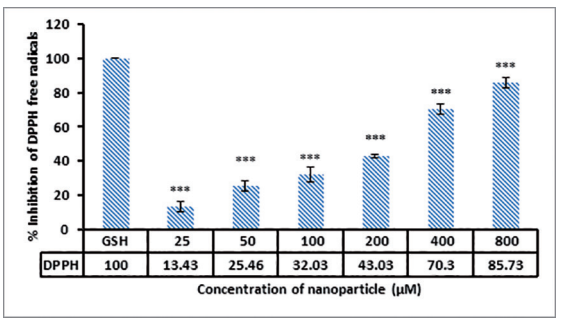

Figure 8: Scavenging capacity of Au-NPs on DPPH free radicals as compared to standard compound (GSH). Data are expressed as mean ± standard division.

The DPPH radical contains an odd electron which is responsible for the absorbance at 517 nm and also for visible deep purple color. When DPPH accepts an electron donated by an antioxidant compound on the surface of

Au-NPs solution, the DPPH is decolorized which can be quantitatively measured from the changes in absorbance.

3.7. ABTS radical scavenging activity

In order to assess the antioxidant activity of biosynthesized nanoparticles, ABTS free radical scavenging activity was studied. Figure 9 displays the NPs has antiradical activity via inhibiting ABTS radical with the IC_{50} value of about 100 µM. Bioformed nanoparticles presented dose dependent activity and the ABTS scavenging effect has been observed 96.83 % at a concentration of 800 µM.

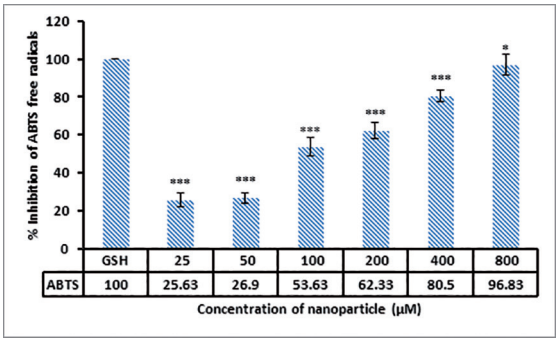

Figure 9: Scavenging capacity of Au-NPs on ABTS free radicals as compared to standard compound (GSH). Data are expressed as mean ± standard division.

4. Conclusion

A green method using *sumac* extract can be used as a safe, simple and economical process for production of gold nanoparticles, without requirement of any chemical reductant or capping agent. The biomolecules present in *sumac* could be potentially acted as an electron donor system and ligand agents to form stabilized nanoparticles. Therefore, using of *sumac* extract will be a new and favorable alternative to the current processes to produce metallic nanoparticles in large scale without generating any toxic byproducts. The bioformed metallic nanoparticles are expected to have potential capacity to use in antioxidant products.

5. Acknowledgment

The authors are thankful to the staff of Universiti Putra Malaysia for their kind support and assistance, especially Department of Bioprocess Technology, Faculty of Biotechnology and Biomolecular Sciences, for the laboratory facilities and technical assistance.

6. References

1. Ferrari M. Cancer nanotechnology: opportunities and challenges. *Nature Reviews Cancer.* 2005;5:161-171.

2. Mahdavi M, Ahmad MB, Haron MJ, Namvar F, Nadi B, Zaki A, et al. Synthesis, surface modification and characterisation of biocompatible magnetic iron oxide nanoparticles for biomedical applications. *Molecules*. 2013;18(7):7533-7548.

3. El-Sayed MA. Some Interesting Properties of Metals Confined in Time and Nanometer Space of Different Shapes. *Accounts of Chemical Research*. 2001;34(4):257-264.

4. Huang X, Jain PK, El-Sayed IH, El-Sayed MA. Determination of the Minimum Temperature Required for Selective Photothermal Destruction of Cancer Cells with the Use of Immunotargeted Gold Nanoparticles. *Photochemistry and Photobiology*. 2006;82(2):412-417.

5. Youngjin K, Johnson RC, Hupp JT. Gold Nanoparticle-Based Sensing of "Spectroscopically Silent" Heavy Metal Ions. *Nano Letters*. 2001;1(4):165-167.

6. Ghosha P, Hana G, Dea M, Kima CK, Rotello VM. Gold nanoparticles in delivery applications. *Advanced Drug Delivery Reviews*. 2008;60(11):1307-1315.

7. Qian W, Murakami M, Ichikawa Y, Che Y. Highly Efficient and Controllable PEGylation of Gold Nanoparticles Prepared by Femtosecond Laser Ablation in Water. *The Journal of Physical Chemistry C*. 2011;115(47):23293-23298.

8. Kumar N, Komarala VK, Dutta V. In-situ synthesis of Au–CdS plasmonic photocatalyst by continuous spray pyrolysis and its visible light photocatalysis. *Chemical Engineering Journal*. 2014;236:66-74.

9. Huang HL, Chen JK, Houng MP. Using soft lithography to fabricate gold nanoparticle patterns for bottom-gate field effect transistors. *Thin Solid Films*. 2012;524:304-308.

10. Azizi S, Namvar F, Mohamad R, Md Tahir P, Mahdavi M. Facile biosynthesis and characterization of palm pollen stabilized ZnO nanoparticles. *Material Letters*. 2015;148:106-109.

11. Alvarez RAB, Cortez-Valadez M, Neira Bueno LO, Britto Hurtado R, Rocha-Rocha O, Delgado-Beleño Y, et al. Vibrational properties of gold nanoparticles obtained by green synthesis. *Physica E: Low-dimensional Systems and Nanostructures*. 2016;84:191-195.

12. Saifuddin N, Wong CW, Nur Yasumira AA. Rapid Biosynthesis of Silver Nanoparticles Using Culture Supernatants of Bacteria With Microwave Irradiation. *Journal of Chemistry*. 2009;6(1):61-70.

13. Vahabi K, Mansoori GA, Karimi S. Biosynthesis of Silver Nanoparticles by Fungus Trichoderma Reesei (A Route for Large-Scale Production of AgNPs). *Insciences Journal*. 2011;1(1):65-79.

14. Schneidewind H, Schüler T, Strelau KK, Weber K, Cialla D, Diegel M, et al. The morphology of silver nanoparticles prepared by enzyme-induced reduction. *Beilstein Journal of Nanotechnology*. 2012;3:404-414.

15. Azizi S, Ahmad MB, Namvar F, Mohamad R. Green biosynthesis and characterization of zinc oxide nanoparticles using brown marine macroalga *Sargassum muticum* aqueous extract. *Material Letters*. 2014;116:275-277.

16. Mahdavi M, Namvar F, Ahmad MB, Mohamad R. Green Biosynthesis and Characterization of Magnetic Iron Oxide (Fe_3O_4) Nanoparticles Using Seaweed (*Sargassum muticum*) Aqueous Extract. *Molecules*. 2013;18:5954-5564.

17. Mavlyanov SM, Islambekov SY, Karimdzhanov AK, Ismailov AI. Polyphenols of the fruits of some varieties of pomegranate growing in Uzbekistan. *Chemistry of Natural Compounds*. 1997;33(1):98-99.

18. Fazeli MR, Amin G, Attari MMA, Ashtiani H, Jamalifar H, Samadi N. Antimicrobial activities of Iranian sumac and avishan-e shirazi (*Zataria multifora*) against some food-borne bacteria. *Food Control*. 2007;18(6):646-649.

19. Duke JA, Bogenschutz-Godwin MJ, duCellier J, Duke PAK. *Handbook of Medicinal Herbs*. Boca Raton: CRC Press; 2002. p. 269-270.

20. Mavlyanov SM, Islambekov SY, Karimdzhanov AK, Ismailov AI. Anthocyans and organic acids of the fruits of some species of sumac. *Chemistry of Natural Compounds*. 1997;33:209.

21. Candan F, Sökmen A. Effects of *Rhus coriaria* L (Anacardiaceae) on lipid peroxidation and free radical scavenging activity. *Phytotherapy Research*. 2004;18(1):84-86.

22. Rajamanikandan S, Sindhu T, Durgapriya D, Sophia D, Ragavendran P, Gopalakrishnan VK. Radical scavenging and antioxidant activity of ethanolic extract of *Mollugo nudicaulis* by *in vitro* assays. *Indian Journal of Pharmaceutical Education and Research*. 2011;45:310-316.

23. Li P, Huo L, Su W, Lu R, Deng C, Liu L, et al. Free radical-scavenging capacity, antioxidant activity and phenolic content of *Pouzolzia zeylanica*. *Journal of the Serbian Chemical Society*. 2011;76(5):709-717.

24. Richard JP. *The Chemistry of Gold*. Amsterdam: Elsevier; 1978.

25. Singaravelu G, Arockiamary JS, Kumar VG, Govindaraju K. A novel extracellular synthesis of monodisperse gold nanoparticles using marine alga, *Sargassum wightii* Greville. *Colloids and Surfaces B: Biointerfaces*. 2007;57(1):97-101.

26. Gardea-Torresdey JL, Gomez E, Peralta-Videa J, Parsons JG, Troiani HE, Santiago P, et al. Alfalfa Sprouts: A Natural Source for the Synthesis of Silver Nanoparticles. *Langmuir*. 2003;19(4):1357-1361.

27. Bandyopadhyay S, Paul GK, Roy R, Sen SK, Sen S. Study of structural and electrical properties of grain-boundary modified ZnO films prepared by sol–gel technique. *Materials Chemistry and Physics*. 2002;74(1):83-91.

28. Falcão L, Araújo MEM. Tannins characterization in historic leathers by complementary analytical techniques ATR-FTIR, UV-Vis and chemical tests. *Journal of Cultural Heritage*. 2012;14(6):499-508.

29. Sangeetha G, Rajeshwari S, Venckatesh R. Green synthesis of zinc oxide nanoparticles by *aloe barbadensis miller* leaf extract: Structure and optical properties. *Materials Research Bulletim*. 2011;46(12):2560-2566.

30. Sanghi R, Verma P. Biomimetic synthesis and characterisation of protein capped silver Nanoparticles. *Bioresource Technology*. 2009;100(1):501-504.

31. Vijayaraghavan K, Mahadevan A, Sathishkumar M, Pavagadhi S, Balasubramanian R. Biosynthesis of Au(0) from Au(III) via biosorption and bioreduction using brown marine alga *Turbinaria conoides*. *Chemical Engineering Journal*. 2011;167(1):223-227.

32. Kumar KP, Paul W, Sharma CP. Green synthesis of gold nanoparticles with *Zingiber officinale* extract: Characterization and blood compatibility. *Process Biochemistry*. 2011;46(10):2007-2013.

33. Ghorbani P, Soltani M, Homayouni-Tabrizi M, Namvar F, Azizi S, Mohammad R, et al. *Sumac* Silver Novel Biodegradable Nano Composite for Bio-Medical Application: Antibacterial Activity. *Molecules*. 2015;20(7):12946-12958.

34. Namvar F, Azizi S, Ahmad MB, Shameli K, Mohamad R, Mahdavi M, et al. Green synthesis and characterization of gold nanoparticles using the marine macroalgae *Sargassum muticum*. *Research on Chemical Intermediates*. 2015;41(8):5723-5730.